ACI STRUCTURAL JOURNAL TECHNICAL PAPER

Title no. 96-S78

Cumulative Seismic Damage of Circular Bridge Columns: Variable Amplitude Tests

by Ashraf El-Bahy, Sashi Kunnath, William Stone, and Andrew Taylor

The findings from an experimental study to investigate cumulative seismic damage in reinforced concrete circular bridge piers is presented. Twelve identical quarter-scale bridge columns, designed in accordance with current AASHTO specifications, were fabricated and tested to failure. Results from Phase I testing, which included constant amplitude tests to determine the low-cycle fatigue characteristics of the bridge column, were presented in a companion paper. This paper summarizes results of variable amplitude testing that focused on the effects of load path on cumulative damage. The imposed displacement histories were obtained from analytical simulations of the model column subjected to a sequence of earthquakes of varying duration and magnitude. Test observations indicate that failure is generally initiated by confinement inadequacy and the rupture of the transverse spiral reinforcement. The tests also demonstrated the potential for low-cycle fatigue fracture of the main longitudinal steel when the specimen was subjected to relatively larger displacement amplitudes, typically in excess of 4 percent lateral drift. A fatigue-based damage model, derived from the constant-amplitude tests completed in Phase I testing, was applied to the observed response of the six specimens tested in this phase. Findings from the study indicate that the energy capacity of members is ductility-dependent and that fatigue-based damage models offer a reliable means of assessing seismic structural performance.

Keywords: bridges (structures); cyclic loads; damage; ductility.

INTRODUCTION

Performance-based design of structures is closely linked to damage limit states. If performance-based design is to eventually become a reality, there is a fundamental need to develop procedures that provide a better estimate of structural performance under expected seismic events. The assessment of performance using damage measures has been suggested as a potential method to achieve this objective, and is regarded by many researchers as a viable and convenient tool if the resulting damage estimates are reliable. Several damage models have been proposed in the literature to evaluate seismic performance. Comprehensive reviews of many of these damage models can be found in recent papers by Powell and Allahabadi[1] and Williams and Sexsmith.[2]

Since seismic loads induce several inelastic cycles at relatively large ductilities combined with innumerable cycles with much smaller deformation demands, the concept of using low-cycle fatigue theories to model damage is logical. A basic prerequisite for developing a fatigue-based model is information on the low-cycle fatigue characteristics of the element or system under consideration. An additional consideration is the treatment of variable amplitude loading that characterizes earthquake-induced structural response. The process of developing a test program that addresses these concerns is a challenge in itself. In a recent paper on the issue of cyclic loading histories to be used in seismic experimentation of structural components, Krawinkler[3] raises the following questions:

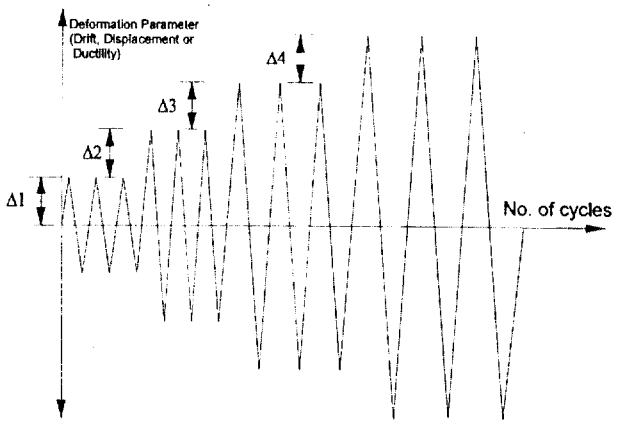

Fig. 1—Typical loading history used in standard cyclic testing.

- How many cycles, what deformation amplitudes, and what sequence of cycles should be employed to evaluate seismic performance?
- How can the results of one experiment under a predetermined loading history be generalized so that conclusions can be drawn on the response of the same component under different loading histories?

It is clear that the issue of determining a load history for use in experimental testing is critical to the overall objective of seismic performance assessment. A review of the past literature on seismic testing indicates that a multiple-step method is the most commonly used type of loading history. The typical loading sequence of a multiple-step test is shown schematically in Fig. 1. The structural assembly or component is first displaced up to a target displacement Δ1. In past testing, this target displacement typically represented the yield displacement of the system. The incremental change to this target value is accomplished in steps, represented in the figure by Δ2, Δ3, etc., and is normally a function of the yield displacement. At least three fully reversed cycles are applied at each target displacement. In more recent tests, there has been a shift towards interstory story drift as the control parameter. In reinforced concrete components, it is important to introduce an elastic cycle between each increase in target displacement to monitor stiffness deterioration.

The multiple-step method of testing provides valuable information on the seismic behavior of the system, but is not suitable for cumulative damage modeling. In particular, it does not consider the effect of load path and the influence of large inelastic

ACI Structural Journal, V. 96, No. 5, September-October 1999.
Received December 22, 1997, and reviewed under Institute publication policies.

ACI member **Ashraf El-Bahy** *is Senior Engineer at Tilden Lobnitz Cooper, Orlando, Fla. He received his PhD from the University of Central Florida, and his BS and MS in civil engineering from Cairo University, Egypt. His research interests include earthquake-resistant design of structures, and inelastic behavior and damage modeling of reinforced concrete.*

ACI member **Sashi Kunnath** *is Associate Professor of Structural Engineering at the University of Central Florida. He received his PhD in structural dynamics and earthquake engineering from the State University of New York, Buffalo, N.Y., and his MS from the Asian Institute of Technology. He is a member of ACI Committees 335, Composite and Hybrid Structures; 369, Seismic Repair and Rehabilitation; and 374, Performance-Based Seismic Design of Concrete Buildings. His research interests include inelastic behavior and damage-based design of concrete structural systems.*

William Stone *is Research Structural Engineer and Leader of the construction metrology and automation group at the National Institute of Standards and Technology, Gaithersburg, Md. He received his PhD from the University of Texas at Austin, Tex., and his BS and MS from Rensselaer Polytechnic Institute. His research interests include structural dynamics, real-time metrology, and robotics and automation in construction.*

ACI member **Andrew Taylor** *is Project Engineer with KPFF Consulting Engineers, Seattle, Wash. He is a member of ACI Committees 341, Earthquake-Resistant Concrete Bridges, and 374, Performance-Based Seismic Design of Concrete Buildings.*

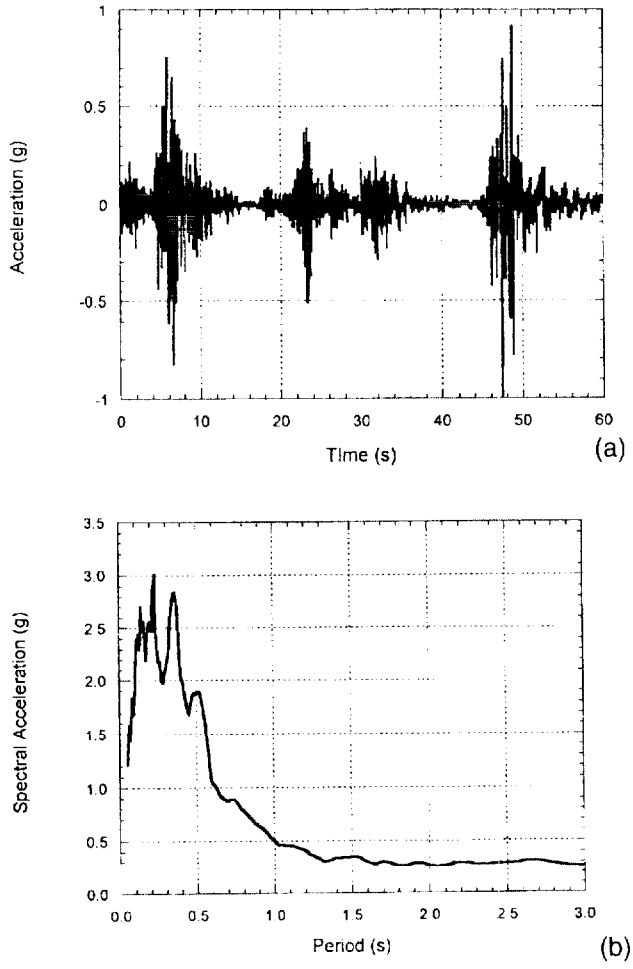

Fig. 2—Earthquake characteristics of imposed loading on Specimens A7 and A8: (a) time history; and (b) acceleration spectra.

cycles on smaller elastic cycles, or vice versa. For example, can it be assumed that an identical system subjected to increasing amplitudes, as represented in Fig. 1, will fail after the same number of cycles if the largest amplitudes were imposed first and followed by smaller amplitudes in reverse order?

The experimental study reported in this paper was designed to specifically address some of the issues raised previously and to provide a basis for the development of a cumulative damage model. Twelve identical quarter-scale circular reinforced concrete columns were tested to failure under different loading histories. The tests were conducted in two phases: Phase I testing, which was reported in a companion paper,[4] consisted of benchmark tests that included characterization of the fatigue behavior of the model columns. In Phase II, another set of six identical specimens were subjected to random displacement histories, the details of which are described in this paper.

RESEARCH SIGNIFICANCE

An alternate test methodology is explored to gain a better understanding of the mechanics of cumulative damage in reinforced concrete (RC) bridge columns. These tests will provide researchers with valuable information on the effects of load path on damage accumulation and the influence of displacement amplitude and ductility on energy dissipation capacity of RC members. The development of cumulative damage models relies on experimental data that include variable amplitudes and a fairly random sequence of application, both of which are considered in the testing program described herein. Finally, the applicability of Miner's linear damage accumulation rule is verified.

DEVELOPMENT OF DISPLACEMENT HISTORIES

A series of over 50 earthquakes, recorded mostly from seismic activity in the west coast of the U. S., was selected for a preliminary study. An analytical model of the bridge pier, calibrated using the force-deformation response from Specimen A2 subjected to standard cyclic test (El-Bahy et al.[4]), was used in a extensive simulation study to obtain the final sequence of displacements. Prior to carrying out the simulation study, a desired sequence of events was chosen. For example, the first specimen was to be subjected to the following sequence of loads:

- A major earthquake causing significant but repairable damage;
- A minor earthquake representing a possible aftershock;
- Another minor event signifying additional earthquakes prior to another major earthquake; and
- A final severe event sufficiently large enough to cause failure of the column.

To achieve such a desired sequence of events and the corresponding damage states, it was necessary to calibrate some measure of damage. A fatigue-based approach was used in which the number of cycles to failure, based on results of the experimental testing in the first phase, formed the basis of defining a certain degree of damage. The elastic cycles were generally ignored in the damage quantification. To illustrate how the procedure was applied in developing the final displacement amplitudes, consider the following situation. An earthquake induces about 30 response cycles, of which only five exceed the yield displacement as follows: three cycles at 4 percent drift, and two cycles at 5.5 percent drift. Based on the results of Phase I testing, the model columns sustained 26 cycles at 4 percent drift, and nine cycles at 5.5 percent drift. Hence, the cumulative damage under the imposed earthquakes was estimated using Miner's linear damage accumulation rule, as follows

$$3/26 + 2/9 = 0.34$$

which is likely to inflict significant damage on the specimen, but is perhaps repairable. A second similar event would certainly damage the specimen beyond repair. To achieve a desired damage scenario, it was necessary to try innumerable combinations. An additional problem in the numerical simulations was the fact that the records were concatenated so as to retain the damaged state and stiffness characteristics at the end of each event. Hence, an earthquake that may have been damaging

Table 1—Ground motions selected for generating random displacement histories for Specimens A7 to A12

Specimen	Event	Description	Purpose	Record	Scale*	PGA, g
A7	1	Damaging earthquake	First major event	Loma Prieta 1989 Presidio	12.00	1.20
	2	Minor earthquake	Aftershock	Imperial Valley 1979 Superstition Mt.	1.80	0.34
	3	Minor earthquake	Second aftershock	San Fernando 1971 2011 Zonal Ave.	1.20	0.10
	4	Severe earthquake	Failure of bridge	San Fernando 1971 455 S. Figueroa St.	3.60	0.54
A8	1	Minor earthquake	Minor damage	Imperial Valley 1979 Superstition Mt.	1.80	0.34
	2	Minor earthquake	Additional damage	San Fernando 1971 2011 Zonal Ave.	1.20	0.10
	3	Damaging earthquake	First major event	Loma Prieta 1989 Presidio	12.00	1.20
	4	Severe earthquake	Failure of bridge	San Fernando 1971 455 S. Figueroa St.	3.60	0.54
A9	1	Major earthquake	First major event	San Fernando 1971 Orion Blvd.	3.25	1.43
	2	Minor earthquake	Aftershock damage	San Fernando 1971 2011 Zonal Ave.	1.20	0.10
	3	Moderate earthquake	Additional damage	El Centro 1940	1.00	0.35
	4	Minor earthquake	Aftershock	San Fernando 1971 455 S. Figueroa St.	1.00	0.15
	5	Severe earthquake	Failure of structure	San Fernando 1971 Orion Blvd.	3.25	1.43
A10	1	Minor earthquake	Minor damage	San Fernando 1971, 2011 Zonal Ave.	1.20	0.10
	2	Moderate earthquake	Additional damage	El Centro 1940	1.00	0.35
	3	Minor earthquake	Aftershock	San Fernando 1971, 455 S. Figueroa St.	1.00	0.15
	4	Major earthquake	First major event	San Fernando 1971, Orion Blvd.	3.25	1.43
	5	Severe earthquake	Failure of structure	San Fernando 1971, Orion Blvd.	3.25	1.43
A11	1	Major event	First damaging earthquake	Northridge 1994, VA Hospital	1.00	0.42
	2	Minor earthquake	Aftershock	Northridge 1994, Griffith Observatory	1.00	0.26
	3	Minor earthquake	Additional damage	Taft 1952	1.00	0.36
	4	Severe earthquake	Failure of Column SCT	Mexico City 1985	1.00	0.17
A12	1	Minor earthquake	Minor damage	Northridge 1994, Griffith Observatory	1.00	0.26
	2	Minor earthquake	Additional damage	Taft 1952	1.00	0.36
	3	Major event	First damaging earthquake	Northridge 1994, VA Hospital	1.00	0.42
	4	Severe earthquake	Failure of column SCT	Mexico City 1985	1.00	0.17

*Multiplying factor on acceleration amplitude.

in the initial state of the structure may not have any significant effect when applied a second time. After many trials, however, including the need to scale some records, it was possible to develop three separate damage scenarios, the details of which are summarized as follows.

Selected ground motions

A total of 10 earthquakes were used in the final simulations for the three separate damage scenarios considered in this study. Each of the three sets of displacements were used twice: during the second usage the sequence of the applied displacements were altered so as to force the system to follow a different load path. Hence, there were truly only three sets of displacement histories used, and each was repeated a second time but applied in a different sequence. Table 1 presents a complete summary of the earthquake records that were applied. The accelerograms and the corresponding spectra used as input motion for simulating the displacement histories for Specimens A7 to A12 are shown in Fig. 2 to 4. Note that the accelerations shown include all the earthquakes selected for a given damage scenario. The analysis was not repeated for the next specimen by rearranging the input motions; rather, the displacements from the first simulation were rearranged to simply alter displacement paths on the assumption that some random combination of ground motions could produce such a displacement path. It is important to remember that one of the primary purposes of the testing is to investigate effects of load paths. Hence, it was essential to use the same total displacement history without introducing additional cycles or altering amplitudes.

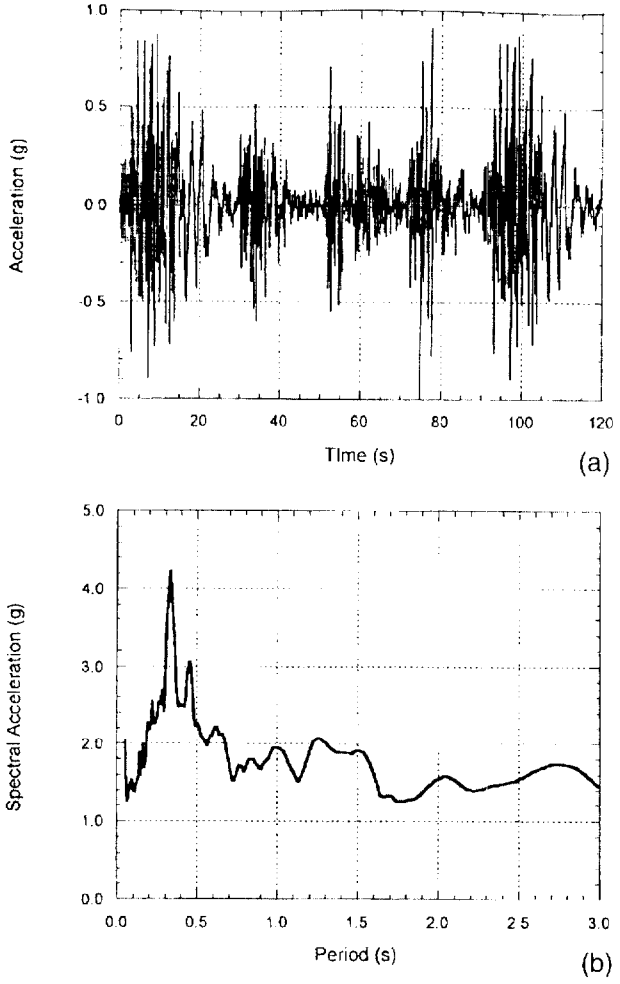

Fig. 3—Earthquake characteristics of imposed loading on Specimens A9 and A10: (a) time history; and (b) acceleration spectra.

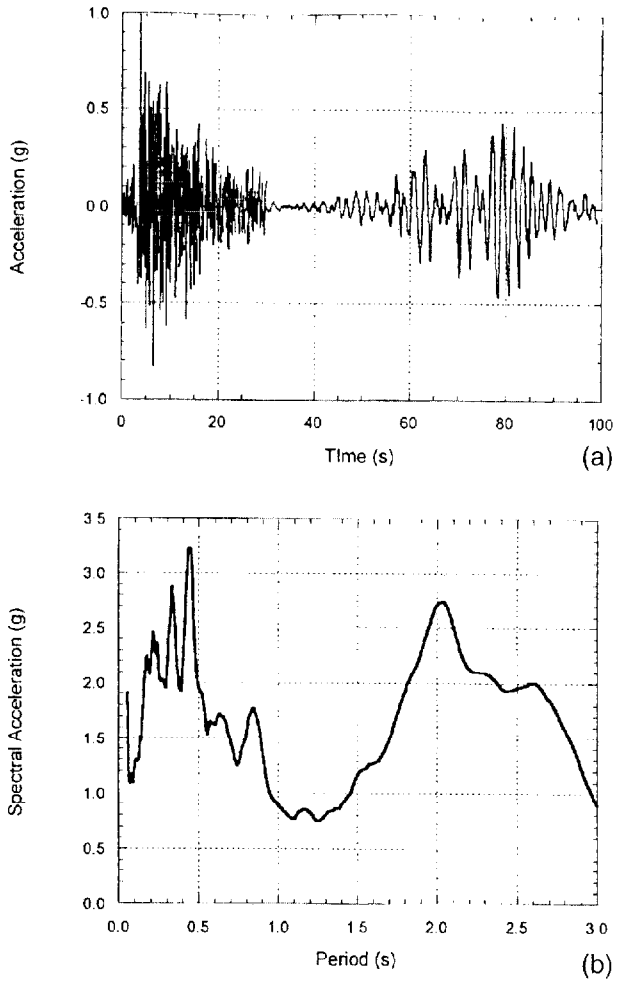

Fig. 4—Earthquake characteristics of imposed loading on Specimens A11 and A12: (a) time history; and (b) acceleration spectra.

Analyses of the model column subjected to the earthquakes shown in Fig. 2 to 4 were carried out using IDARC.[5] Additional information on the analytical simulation, model verification, and development of the random displacement histories can be found in Kunnath et al.[6]

RESULTS OF VARIABLE AMPLITUDE TESTING

The six specimens tested in this series were labeled A7 through A12. Details of the test setup and instrumentation were reported in the first installment of this two-part paper.[4] The imposed displacement histories represent analytically computed inelastic response of the model column subjected to the earthquake motions listed in Table 1. As in the case of the first six specimens tested in Phase I, all column tests reported herein were performed with a constant axial force equal to $0.1 f'_c A_g$.

Specimen A7

Specimen A7 was subjected to variable amplitude displacement cycles generated from four different earthquakes. The first record produced significant displacements that were considered sufficient to induce moderate damage to the specimen. The next two earthquakes were meant to represent aftershocks and/or other minor events that do not result in additional significant damage. The final ground motion was selected to produce severe damage and probable failure of the system.

The first set of imposed displacements caused significant cracking and initiated spalling at a drift of approximately 1.75 percent after 46 half-cycles of loading. Before Cycle 32 was completed, the specimen had undergone one complete cycle at a drift amplitude of approximately 5 percent. At this point, some buckling of the longitudinal bars was observed on one side of the specimen. The next 40 cycles were uneventful since they were composed of elastic cycles with drifts under 0.5 percent. At half-cycle No. 145, which was part of the second earthquake, the spalling had stabilized and the slightly buckled longitudinal bars were clearly visible. By the end of the third earthquake, at which time 94 full cycles of displacement were applied, there was no evidence of further deterioration, though it contained 1-1/2 cycles of 2.5 percent drift. No further extension of the plastic hinge length, which stabilized at approximately 150 mm, was observed. Measured crack widths were between 2.5 to 4 mm. Finally, at half-cycle No. 269, and with a drift of almost 6 percent, failure of the specimen was recorded following the rupture of a spiral in the plastic hinge zone. This occurred during the peak displacement demand of the fourth earthquake. In all, the specimen had undergone about eight inelastic cycles of displacement at an average drift of approximately 3.6 percent. The applied displacement history and the resulting force-deformation hysteresis are shown in Fig. 5 and 6, respectively.

Specimen A8

The total displacement history imposed on Specimen A8 was essentially the same as that used in Specimen A7, but the sequence of events was changed (Table 1). The two minor events were applied first, followed by the two major earthquakes. Consequently, visible cracking and spalling was not evident until half-cycle No. 114. The spirals and longitudinal reinforcing bars

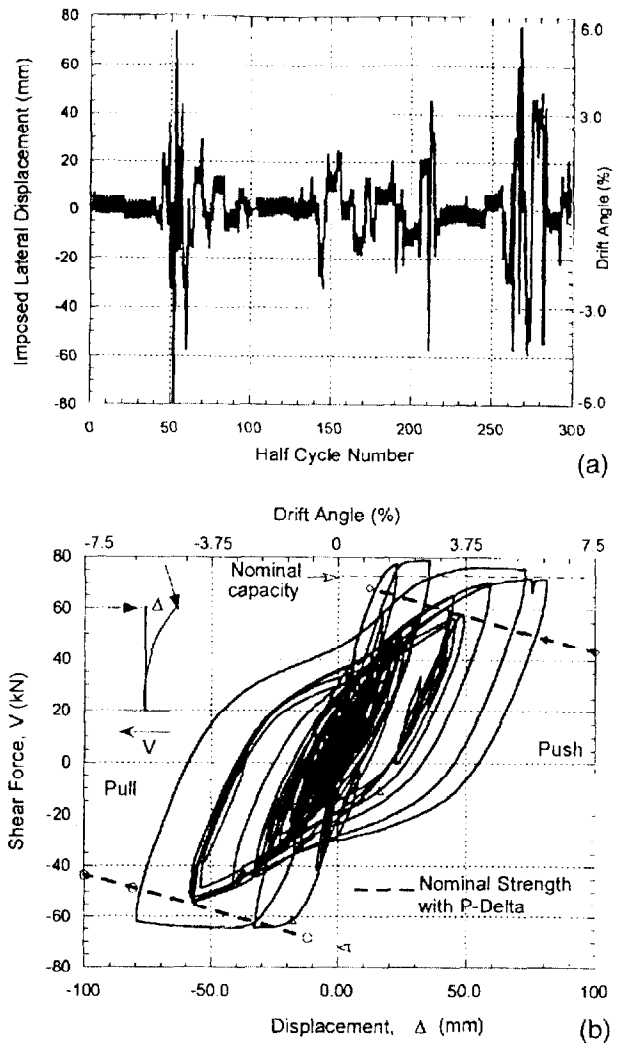

Fig. 5—Behavior of Specimen A7 to random amplitude loading: (a) imposed displacement history; and (b) shear-drift response.

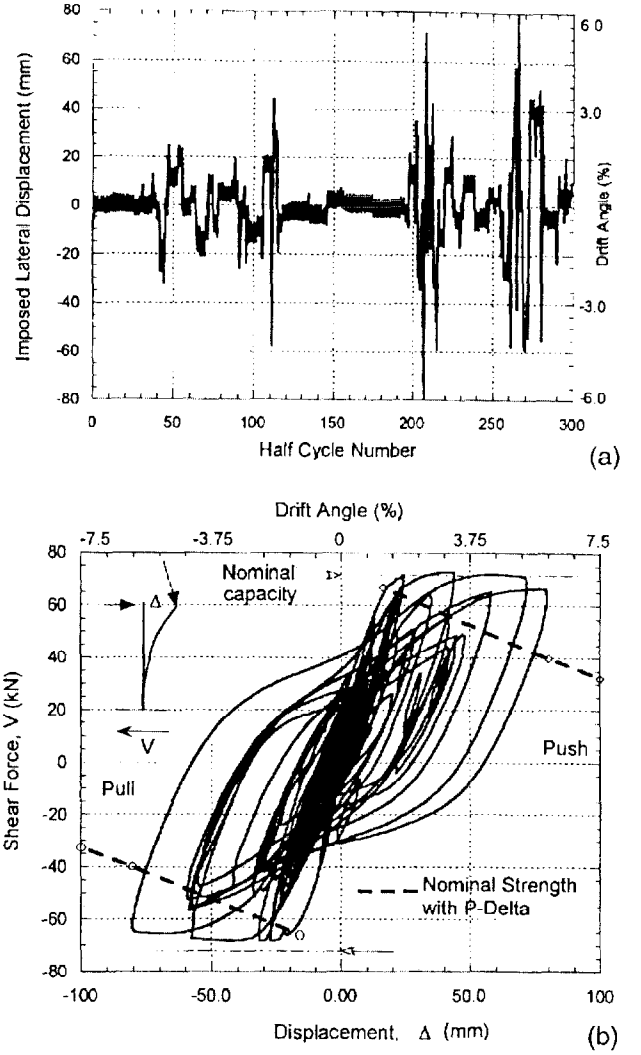

Fig. 6—Behavior of Specimen A8 to random amplitude loading: (a) imposed displacement history; and (b) shear-drift response.

were exposed along the plastic hinge zone after 104 full cycles (or half-cycle No. 209). Some buckling of the longitudinal bars was noticed towards the end of half-cycle No. 220 following a few inelastic cycles at drifts exceeding 2.5 percent. At half-cycle No. 267, during the peak displacement demand of earthquake No. 4, necking of one of the spiral bands was observed. In the next cycle, at approximately the same cycle at which failure occurred in Specimen A7, rupture of the spiral reinforcement took place. The sequence of the imposed displacements and the resulting force-deformation response is shown in Fig. 6.

Specimen A9

Column A9 was tested under simulated random displacements resulting from a series of five different earthquakes (Table 1). A fifth earthquake was used in this specimen to introduce additional small amplitude cycles between two large events.

The first significant crack was observed on the tension side of the specimen at half-cycle No. 29 (approximately 14 full cycles) when the lateral drift reached 2 percent. First spalling occurred at half-cycle No. 49 during the first earthquake, accompanied by major crack propagation. After nearly five inelastic cycles at an average drift of 3.0 percent, the crack widths had reached approximately 2.0 mm. The next two earthquakes did not produce any significant damage since all of the imposed drifts remained less than 1.5 percent. Earthquake No. 4 was of moderate intensity and was composed of approximately two inelastic cycles at a drift of approximately 2.5 percent. By the end of this event, at half-cycle No. 190, minor buckling was noted in the longitudinal bars. However, it appeared that the specimen was still repairable. The buckling of longitudinal bars increased and became more prominent during half-cycle No. 240 of the fifth and final earthquake. At half-cycle No. 260, at an imposed drift exceeding 5.5 percent, confinement failure occurred with the rupture of a spiral. The plastic hinge length was measured as approximately 200 mm towards the end of testing. The displacement history applied to Specimen A9 and the base shear versus lateral-displacement response of the bridge column is plotted in Fig. 7.

Specimen A10

Specimen A10 was subjected to essentially the same displacement history as Specimen A9, but the sequence of applied displacements was altered. The objective of altering only the sequence of loading was to monitor the effect of load path on the capacity of the specimen. A similar test conducted on Specimen A8 did not reveal any significant influence of load path, but, in this test, a larger number of low-amplitude cycles were introduced between cycles of larger amplitudes.

Earthquake No. 1 caused minor cracking and initiated spalling, but the overall damage was cosmetic. The second earthquake, like the first, induced only one significant cycle of displacement that resulted in a lateral drift of approximately

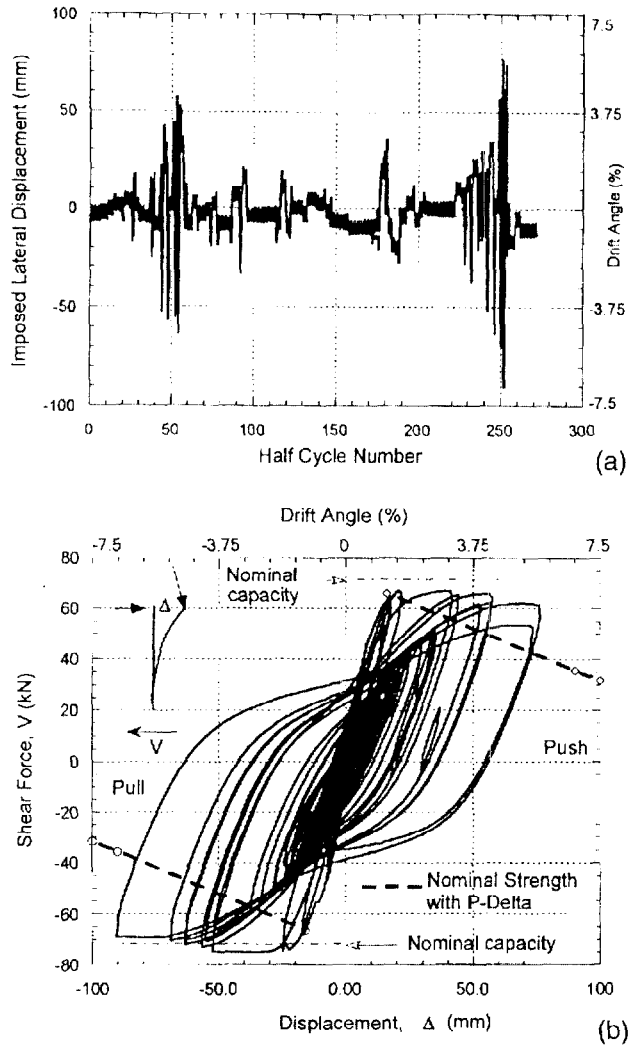

Fig. 7—Behavior of Specimen A9 to random amplitude loading: (a) imposed displacement history; and (b) shear-drift response.

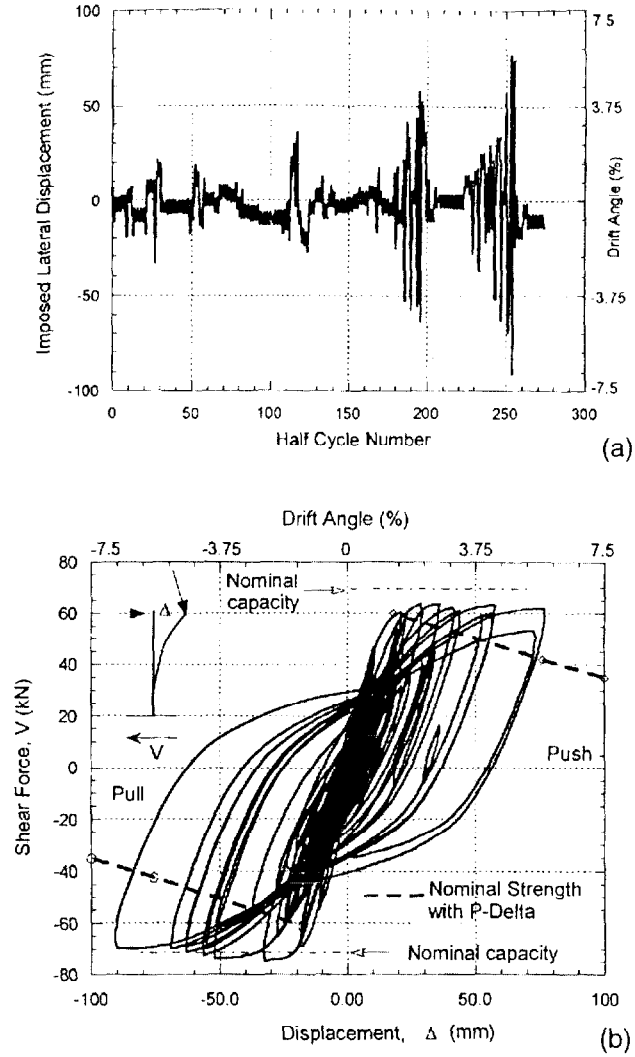

Fig. 8—Behavior of Specimen A10 to random amplitude loading: (a) imposed displacement history; and (b) shear-drift response.

2 percent. At half-cycle No. 121, which was part of the third earthquake, significant spalling of the cover was observed. The damage at the end of earthquake No. 4 was considered repairable. Significant buckling of the central longitudinal bar was recorded during half-cycle No. 258 at a lateral drift in excess of 6 percent, which was part of the peak displacement amplitude of earthquake No. 5. Accompanying this was some necking of the spirals—a normal consequence of longitudinal bar buckling. The very next cycle resulted in failure of one of the spirals. The plastic hinge length was estimated between 190 and 200 mm. The observed column response is presented in Fig. 8.

Specimen A11

An effort was made to introduce larger amplitude cycles for the final pair of specimens with the objective of inducing a low-cycle fatigue failure of the longitudinal bar as observed in the constant-amplitude phase of testing. The Mexico City earthquake of 1985 proved to be an ideal choice. The remaining earthquakes used in this simulation are shown in Table 1.

First cracking and minor spalling was observed at half-cycle No. 27. By half-cycle No. 38, concrete spalling had extended to indicate extension of the plastic hinge zone, and cracks had propagated 75 to 100 mm above the hinge zone. The maximum crack width was approximately 2 mm, which increased to almost 4 mm following the half-cycle No. 42. The next two earthquakes that represented potential aftershocks did not cause any further damage to the column. The final earthquake imposed several large displacement cycles in excess of 3.5 percent drift combined with a single cycle of approximately 7 percent drift. Buckling of the longitudinal bars was observed at half-cycle No. 252 on both sides of the specimen. Two spirals failed in consecutive half-cycles (No. 270 and 271). The final plastic hinge length was approximately 220 mm. The specimen was further loaded for the remainder of the earthquake until fracture of a longitudinal bar was recorded at half-cycle No. 275. The imposed displacement and recorded force-displacement behavior is shown in Fig. 9.

Specimen A12

The largest amplitudes were imposed by earthquake No. 1 on Specimen A11, which failed midway through earthquake No. 4. For Specimen A12, the displacement cycles corresponding to earthquake No. 4 up to failure of the column were first applied, followed by the two minor earthquakes, followed by earthquake No. 1, and then followed by the remainder of earthquake No. 4. Hence, the largest amplitudes were reserved for the final cycles. Since all the previous specimens failed in confinement, it was of interest to see if the longitudinal bar fracture could be induced through an alternate sequence of cycling.

The specimen experienced a couple of cycles at 2 percent lateral drift prior to spalling and visible crack propagation. The

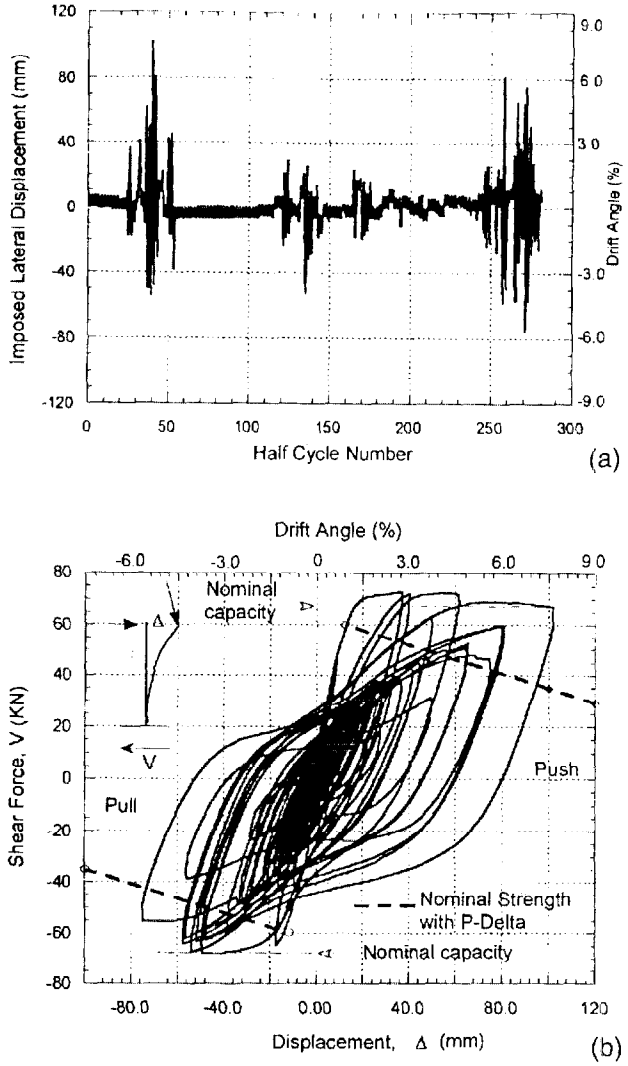

Fig. 9—Behavior of Specimen A11 to random amplitude loading: (a) imposed displacement history; and (b) shear-drift response.

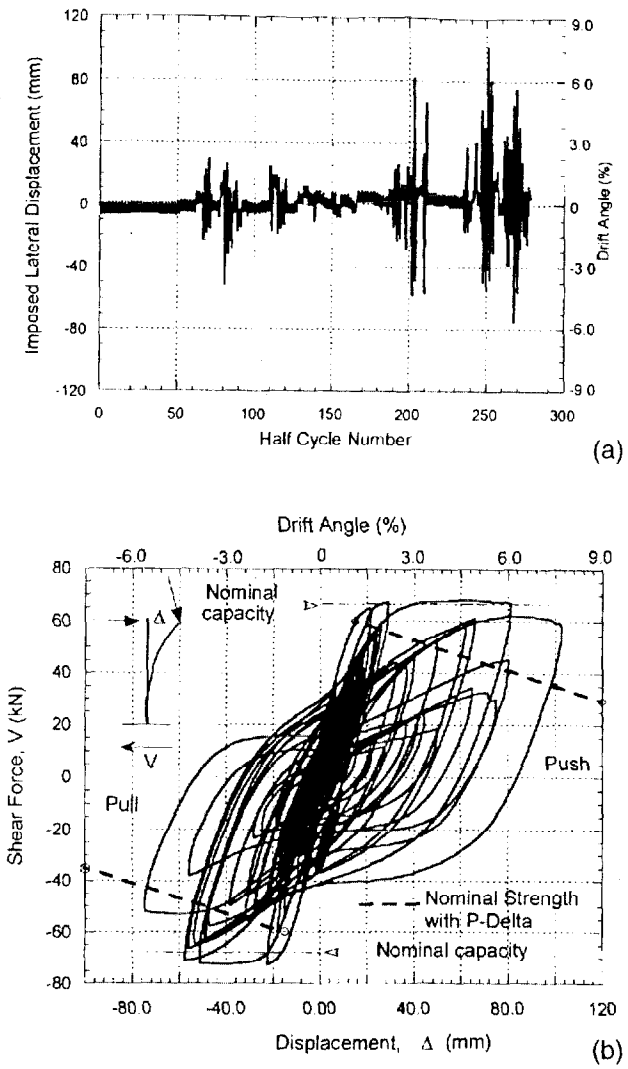

Fig. 10—Behavior of Specimen A12 to random amplitude loading: (a) imposed displacement history; and (b) shear-drift response.

second earthquake, which did not contain any large amplitude cycles, did no further damage to the column. At the onset of the large amplitude cycles due to earthquake No. 3, corresponding to half-cycles No. 205 and 206, significant spalling was observed on both sides of the specimen. At this time, the column had undergone one large inelastic excursion with a lateral drift of almost 6 percent. The average crack width was about 3.0 mm. Buckling of the longitudinal bars was first noticed at half-cycle No. 254, leading to a kink (or necking) in the spirals. First signs of failure were recorded during the fourth earthquake at half-cycle No. 255, when one of the spirals ruptured. The maximum lateral drift at this cycle exceeded 7 percent lateral drift, and the plastic hinge length was approximately 200 mm. It was decided to continue loading Column A12 with the rest of the displacement history. Finally, one of the longitudinal bars fractured at half-cycle No. 276 at approximately the same cycle as the previous specimen. The applied displacements and the observed force-deformation response are displayed in Fig. 10.

DAMAGE MODELING

The constant-amplitude testing reported in the companion paper[4] yielded the following fatigue-life relationship for the columns tested in this study

$$\delta(\text{percent}) = 10.6(N_{2f})^{-0.285} \quad (1)$$

where δ is the lateral drift, and N_{2f} is the number of complete cycles to failure. It is possible to define cumulative damage using Miner's linear damage rule, as follows

$$D = \sum \frac{1}{N_{2f}} \quad (2)$$

where N_{2f} is computed for each imposed drift amplitude using Eq. (1), and the summation is performed over the entire cyclic history. The application of the previously mentioned damage measure produced the damage history curves shown in Fig. 11. It can be stated that the computed damage is in reasonable agreement with test observations. Specimens A7 through A10 indicate damage of approximately 0.8 that, at best, may be considered irreparable damage, while Specimens A11 and A12 are closer to collapse.

SUMMARY OF FINDINGS

It is recommended that the reader review the findings from Phase I testing that were reported in an earlier paper[4] since some of the statements made herein are partly based on the collective findings of both phases of testing.

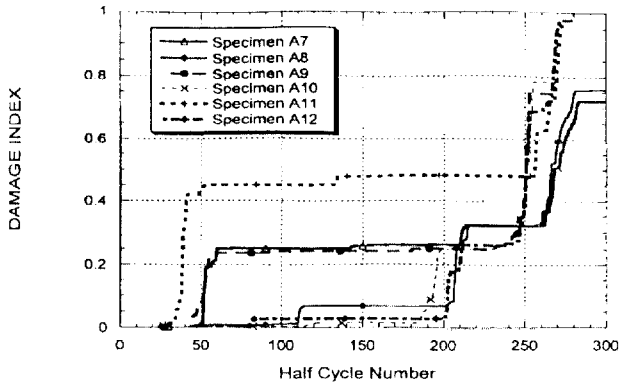

Fig. 11—Computed damage history of columns subjected to random displacement amplitudes using proposed fatigue damage model.

Table 2—Correlation of damage limit states with visual observations

Damage indicator	Damage state	Description	Visual observation based on current testing
N	None	No visible damage, either cosmetic or structural	No visible cracks
I	Insignificant	Damage requires no more than cosmetic repair. No structural repairs necessary	Hairline cracks; minor spalling; no exposed reinforcement
M	Moderate	Repairable structural damage has occurred. Existing elements can be repaired essentially in place, without substantial demolition or replacement of elements	Excessive spalling; exposed reinforcement; no buckling of longitudinal bars; no necking of spirals
H	Heavy	Damage is so extensive that repair of elements is either not feasible or requires major demolition or replacement	Buckling/fracture of longitudinal bars; necking/rupture of spirals

Phase I testing clearly demonstrated that energy capacity is a function of the displacement amplitude to which the specimen is subjected. However, this phase of testing, which consisted primarily of variable amplitude testing, indicates that the average energy capacity is reasonably predicted by a standard cyclic test (Fig. 12). It is still important to determine the number and amplitude of inelastic cycles if energy-based measures are used to predict damage.

As in the previous phase of testing, it was found that the plastic hinge length is not only a function of the largest displacement amplitude to which the specimen is subjected but also the sequence of inelastic reversals. The hinge length appears to stabilize after several initial inelastic cycles and may not be influenced by future displacements. This would mean that a bridge column that experiences the largest displacement amplitude in the first few cycles would develop a larger hinge length than a similar column that experiences several smaller inelastic reversals prior to the largest amplitude.

Failure in all of the bridge columns was initiated by confinement loss following the rupture of the hoop spiral in the plastic hinge zone. The most significant distress to the longitudinal bars occurred in Specimens A11 and A12, which experienced the largest drift amplitudes of all tested specimens. Low-cycle fatigue fracture was imminent in these specimens, as was verified by the additional cycles imposed following

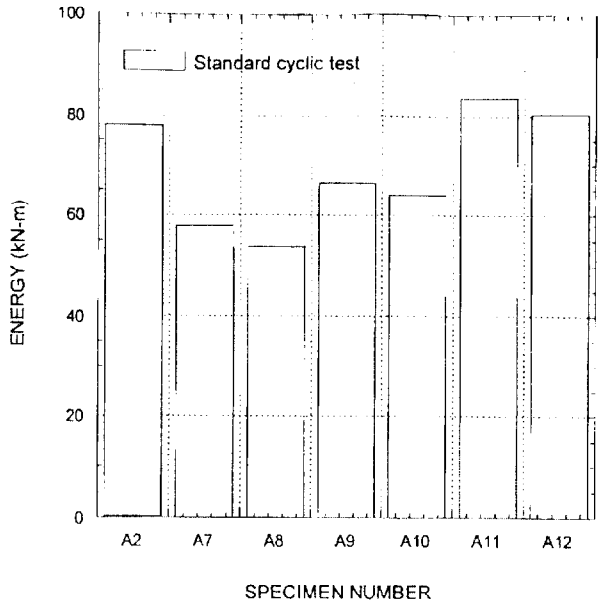

Fig. 12—Dissipated energy at failure of specimens subjected to random displacement amplitudes.

hoop failure. The somewhat premature failure of the hoops can be attributed to the fracture energy of the annealed hoop steel, which was approximately 20 percent lower than comparable normal reinforcing bars (Phase I test results[4]).

Finally, in an attempt to correlate visually observed damage during testing with damage limit states, all recorded test data were evaluated carefully to develop a correlation chart. This chart, presented in Table 2, provides a convenient aid in post-earthquake reconnaissance evaluation of structural safety.

To conclude, this research effort was directed towards gaining a better understanding of the cumulative damage process and can be viewed as an attempt to develop a systematic test program to calibrate a damage-based procedure for seismic design of bridge columns. Only flexural failure modes were considered in this study, and the findings reported herein are limited to the scope of the design and test parameters considered.

ACKNOWLEDGMENTS

Financial support for this project provided by the National Center for Earthquake Engineering Research (NCEER), the Federal Highway Administration (FHWA), and the California Department of Transportation (CALTRANS) is gratefully acknowledged. Special thanks are due to the technical staff of the Structural Testing Laboratory at the National Institute of Standards and Technology: Steve Johnson, Frank Rankin, Erik Anderson, Max Peltz, and James Little for their assistance during the experimental testing.

CONVERSION FACTORS

1 mm = 0.0394 in.
1 m = 3.28 ft
1 mm^2 = 0.00155 in.^{2}
1 MPa = 145 psi
1 kN = 0.225 kip-force

NOTATIONS

A_g = gross area of column section
f'_c = unconfined concrete compressive stress
N_{sf} = number of complete cycles to failure
δ = lateral drift
Δ = deformation parameter (displacement, ductility, or drift)

REFERENCES

1. Williams, M. S., and Sexsmith, R. G., "Review of Methods Assessing Seismic Damage in Concrete Structures," *Technical Report* 94-02, Earthquake Engineering Research Facility, University of British Columbia, 1994.

2. Powell, G., and Allahabadi, R., "Seismic Damage Prediction by Deterministic Methods: Concepts and Procedures," *Earthquake Engineering and Structural Dynamics*, V. 16, 1988.

3. Krawinkler, H., "Cyclic Loading Histories for Seismic Experimentation on Structural Components," *Earthquake Spectra*, V. 12, No. 1, Jan. 12, 1996.

4. El-Bahy, A.; Kunnath, S. K.; Taylor, A. W.; and Stone, W. C., "Cumulative Seismic Damage of Circular Bridge Columns: Benchmark and Constant Amplitude Tests," *ACI Structural Journal*, V. 96, No. 4, July-Aug. 1999, pp. 633-641.

5. Kunnath, S. K.; Reinhorn, A. M.; and Lobo, R. F., "IDARC: Inelastic Damage Analysis of RC Structures—Version 3.0," *Report* NCEER-92-0022, State University of New York at Buffalo, 1992.

6. Kunnath, S. K.; El-Bahy, A.; Taylor, A.; and Stone, W. C., "Cumulative Seismic Damage of Reinforced Concrete Bridge Piers," *Report* NCEER-97-0006, State University of New York at Buffalo.